Antitumor activity of a 2-pyridinecarboxaldehyde 2-pyridinecarboxylic acid hydrazone copper complex and the related mechanism

YINGLI YANG[1], TENGFEI HUANG[1], SUFENG ZHOU[2], YUN FU[1], YOUXUN LIU[1], YANBIN YUAN[3], QIONGQING ZHANG[1], SHAOSHAN LI[3] and CHANGZHENG LI[1]

[1]Department of Molecular Biology and Biochemistry, and [2]Clinical Skill Training Center, Xinxiang Medical University; [3]Department of Surgery, The Third Affiliated Hospital of Xinxiang Medical University, Xinxiang, Henan, P.R. China

Received April 21, 2015; Accepted June 8, 2015

DOI: 10.3892/or.2015.4087

Abstract. In the present study, 2-pyridinecarboxaldehyde 2-pyridinecarboxylic acid hydrazone (PPAH) was prepared and its antitumor activity was evaluated. The inhibition of proliferation of PPAH against the HepG2 and HCT-116 cell lines was less effective, yet in the presence of copper ions, the mixture demonstrated excellent antitumor activity (IC_{50} at 2.75±0.30 μM for the HepG2 cell line, and 1.90±0.20 μM for the HCT-116 cell line, respectively) and the new active species was confirmed to be a PPAH copper complex with a 1:1 ratio by spectral analysis. The excellent antitumor activity of the copper complex prompted us to investigate the underlying mechanism. RT-PCR was performed to detect the changes in the expression of apoptotic genes induced by PPAH and its copper complex. However, no changes were observed when the cells were treated by the agents for 24 or 48 h, indicating that ROS were unlikely involved. Cell cycle analysis showed that both PPAH and its copper complex led to S phase arrest of the cells. The sDNA relaxation assay revealed that the PPAH-copper complex displayed dual topoisomerase inhibition for type I and II. The data suggest that the inhibition of proliferation exhibited by the PPAH copper complex may stem from its dual topoisomerase inhibition, which is rarely observed for a metal complex.

Correspondence to: Dr Changzheng Li, Department of Molecular Biology and Biochemistry, Xinxiang Medical University, East 601 Jinsui Road, Xinxiang, Henan, P.R. China
E-mail: changzhenl@yahoo.com

Dr Shaoshan Li, Department of Surgery, The Third University Hospital, Xinxiang Medical University, East 601 Jinsui Road, Xinxiang, Henan, P.R. China
E-mail: shaoshanlioo1@sina.com

Key words: 2-pyridinecarboxaldehyde 2-pyridinecarboxylic acid hydrazone, antitumor activity, topoisomerase inhibition, copper complex

Introduction

Cancer is a serious health issue that accounts for millions of deaths. In general, localized cancer can be resected by surgery, yet metastatic cancer requires systemic treatment with chemotherapy (1). However, the genetic cytotoxic side-effects and resistance of chemotherapeutic agents used in the clinic have motivated scientists to identify and develop new drugs to replace the currently used arsenal of agents. Different strategies based on tumor cell characteristics, the targeting of specific enzymes or transcription factors, have been proposed in drug development. It is known that neoplastic cells have a higher requirement for iron due to their significantly elevated expression of the transferrin receptor 1 and ribonucleotide reductase (2). In addition, cancer cells take up more copper (Cu) than normal cells and use this metal for angiogenesis and metastasis (3). Due to the crucial roles of these metals, the development of novel Fe and Cu chelators has become a promising anticancer strategy (4).

Hydrazones have been intensively investigated in view of their potential application as anticancer, antiviral, antibacterial and antifungal agents. Pyridinecarboxylic acid hydrazide and pyridinecarboxaldehyde are widely used in the preparation of hydrazone or Schiff base for their potent metal chelating ability. Pyridoxaldehyde isonicotinoyl hydrazone has been extensively evaluated as an antiproliferative agent and iron chelator (5,6). In contrast, these hydrazones have versatile ability in metal. For instance, the metal complex of N-heteroaromatic hydrazones of 2-pyridinecarboxaldehyde often exhibits greater biological activity compared to the corresponding free ligands, with copper(II) complexes being the most active among all the tested complexes (7). However, the underlying mechanisms of the hydrazones and their metal complexes in regards to their anticancer activity are poorly understood. Concerning iron chelators, one hypothesis frequently cited is the inhibition of ribonucleotide reductase, which contains iron at its catalytic center (8). Chelators also exert cytotoxic effects via redox cycling of bound metals and attendant production of free radicals (9,10). Thus, they are involved in an apoptotic response by activating the mitochondrial pathway (11).

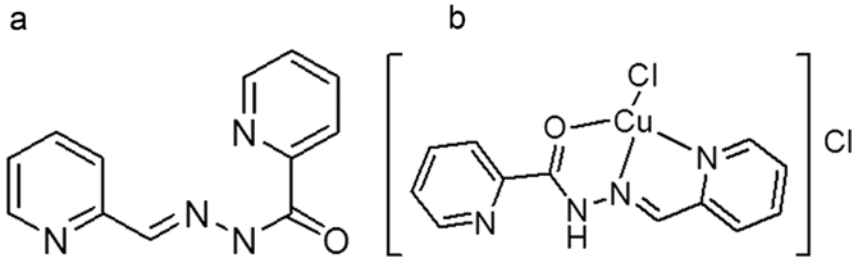

Figure 1. Chemical structures of (a) PPAH and (b) its copper complex. PPAH, 2-pyridinecarboxaldehyde 2-pyridinecarboxylic acid hydrazone.

The excellent biological activities of the hydrazones and their metal complexes prompted us to probe their mechanisms of action. As an extended study, the hydrazone of 2-pyridinecarboxaldehyde 2-pyridinecarboxylic acid hydrazone (PPAH) was prepared and its tumor proliferation inhibition was evaluated. In view of a possible synergistic effect in combination with metal ions, the inhibitory effect on cell proliferation of PPAH in the presence of copper ions was also investigated. Beyond our expectation, the mixture of PPAH with copper displayed excellent proliferation inhibition, which motivated us to probe the underlying mechanism. Thus, the composition of the active species, cell cycle analysis, RT-PCR, comet assay and topoisomerase (Top) inhibition assay were performed. The results revealed that PPAH formed a complex with copper and acted as a novel Top inhibitor for both type I and II, which is rarely observed for metal complexes.

Materials and methods

All reactants and solvents were AR grade. MTT, ethidium bromide (EB), RPMI-1640 medium and agarose were purchased from Sigma.

Preparation of PPAH. 2-Pyridinecarboxylic acid hydrazide was prepared based on a previously reported procedure (12). PPAH was made by refluxing an equal molar ratio of 2-pyridinecarboxylic acid hydrazide and 2-pyridinecarboxaldehyde in ethanol, and the reaction process was monitored by TLC. Pure PPAH was isolated by removing the solvent and re-crystallization in acetonitrile. The ^{1}HNMR (DMSO-d6, Bruker 400 MHz) of PPAH: ^{1}HNMR: 12.54(s, H(N-H)), 8.73(d), 8.70(s, (CHO)), 8.62(d), 8.15(d), 8.06(t), 8.0(d), 7.90(t), 7.70(t), 7.43(t). ^{13}CNMR(ppm): 161.26, 158.36, 149.97, 149.86, 149.78, 149.03, 138.55, 137.35, 127.65, 124.92, 123.37, 120.45. M/Z: 227.2734 $(M+H)^{+}$. The structures of PPAH and its copper complex are shown in Fig. 1.

Determination of the molar ratio of PPAH to copper(II). The molar ratio of PPAH/copper(II) was determined by spectral methods as previously described (13). Briefly, the stock solutions of 1 mM PPAH in 15% dimethylsulfoxide (DMSO) and 1 mM $CuCl_2$ in water were prepared. Next, 0.2 ml of the $CuCl_2$ solution was added to a series of 5-ml volumetric flasks, and then 40, 80, 120, 160, 200, 240, 280, 320, 360 or 400 μl of PPAH was transferred to each flask, respectively. Finally, water was added (5 ml). After mixing and equilibrium, the spectra were recorded on a Shimadzu UV-2450 spectrophotometer.

Cell culture and cytotoxicity assay. The stock solution of PPAH (10 mM) was prepared in 25% DMSO, and was diluted to the required concentration with water when used. The copper complex was made by mixing PPAH with a high concentration of $CuCl_2$ based on 1:1 molar ratio and diluted to the required concentration with water. The human colorectal carcinoma cell line (HCT-116) and liver carcinoma cells (HepG2) were cultured in RPMI-1640 medium supplemented with 10% fetal calf serum (FCS) and antibiotics. The cells collected during the exponential phase of growth ($1x10^4$/ml) were seeded equivalently into 96-well plates, and 1 μl of PPAH or its copper complex at varied concentrations was added after the cells adhered. Following a 48-h incubation at 37˚C in a humidified atmosphere of 5% CO_2, 10 μl MTT solution (1 mg/ml) was added to each well, followed by further incubation for 4 h. The cell culture was removed by aspiration, and 100 μl/well of DMSO was added to dissolve the formazan crystals. The measurement of the absorbance of the solution that was related to the number of living cells was performed on a microplate reader (MK3; Thermo Scientific) at 570 nm. Percent growth inhibition was defined as the percentage of the decrease in absorbance to the appropriate absorbance for each cell line. The same assay was performed in triplet.

Comet assay. The comet assay was adapted as previously described (14). HepG2 cells were treated with or without the investigated compounds (40 and 80 μM for PPAH or 2.5 and 5 μM for the PPAH-Cu complex) followed by a 48-h incubation in a humidified atmosphere of 5% CO_2. The cells were harvested by centrifugation after trypsinization and then embedded in 0.5% low melting point agarose at a final concentration of $1x10^4$ cells/ml. A 20-μl aliquot of this cellular suspension was then spread onto duplicate frosted slides that had previously been covered with 1% normal melting point agarose as a basal layer. The slides were allowed to solidify for 10 min at 4˚C before being placed in lysis buffer for 1 h [2.5 M NaCl, 0.1 M ethylenediaminetetraacetic acid (EDTA), 0.01 M Tris, 1% Triton X-100, 10% DMSO, pH 10.0). After lysis, the slides were transferred into alkaline buffer for 40 min (0.001 M EDTA, 0.3 M NaOH, pH >13.0) to allow the DNA to unwind before migration at 0.66 V/cm and 300 mA for 30 min. All these steps were performed in the dark. After neutralization in 0.4 M Tris-HCl pH 7.4, the slides were stored at 4˚C until analysis following 24 h. Before analysis, the slides were stained with EB (20 μg/ml) and covered with a coverslip. Images was captured using fluorescence microscopy.

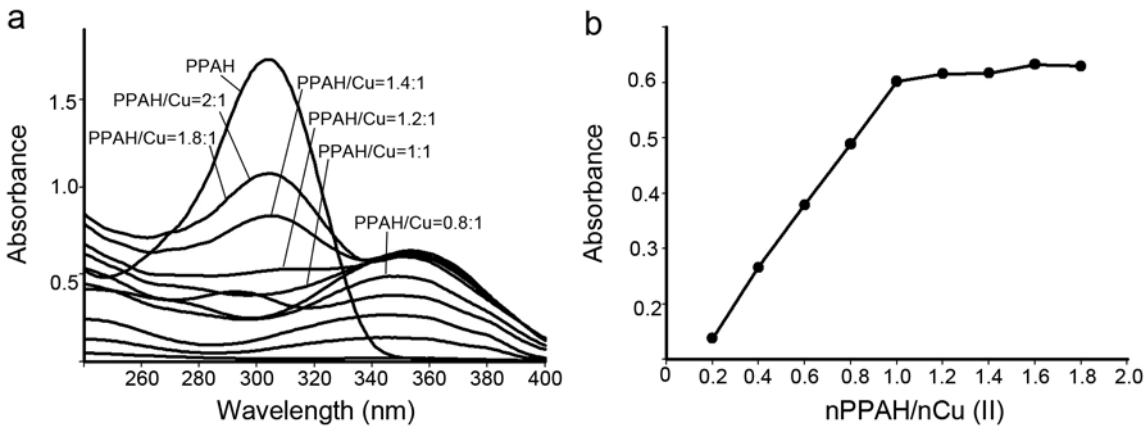

Figure 2. UV-visible spectra of the PPAH copper complex and the relation between absorbance and molar ratio. (a) Spectra of $CuCl_2$ and in the presence of varied concentrations of PPAH; the molar ratio as indicated in the figure. (b) Plot of the absorbance of the copper complex at 350 nm vs. the molar ratio of PPAH/Cu(II); a 1:1 ratio is shown. PPAH, 2-pyridinecarboxaldehyde 2-pyridinecarboxylic acid hydrazone.

RT-PCR. Total RNA was extracted from the cells following treatment with the investigated agents for 24 (or 48 h) using TRIzol reagent (Sangon, Shanghai, China) according to the manufacturer's protocol. Two micrograms of total RNA were used for reverse transcription in a total volume of 20 μl with the M-MLV reverse transcriptase system (LifeFeng Biological Technology Corporation, Shanghai, China). Two microliters of cDNA were subsequently amplified in a total volume of 20 μl using the 2X Taq PCR kit (LifeFeng Biological Technology Corporation) following the conditions recommended by the manufacturer. The sense and antisense primers (synthesized by Shanghai Generay Biological Engineering Corporation, Co., Shanghai, China) for β-actin were: 5'-ACACTGTGCCC ATCTACGAGG-3' and 5'-CGGACTCGTCATACTCCTG CT-3' (615 bp) used as an internal control; the sense and antisense primers for caspase 3 were: 5'-GAAGCGAATC AATGGACTCTGG-3' and 5'-ACATCACGCATCAATTCCA CAA-3' (241 bp); the sense and antisense primers for caspase 8 were: 5'-AAGTTCCTGAGCCTGGACTACAT-3' and 5'-ATTT GAGCCCTGCCTGGTGTCT-3' (227 bp); the sense and antisense primers for p53 were: 5'-GTCTACCTCCCGCCAT AA-3' and 5'-CATCTCCCAAACATCCCT-3' (316 bp); the sense and antisense primers for bcl were: 5'-TTACCAAGCAG CCGAAGA-3' and 5'-TCCCTCCTTTACATTCACAA-3' (309 bp); the sense and antisense primers for bax were: 5'-TTT TGCTTCAGGGTTTCATC-3' and 5'-GGCCTTGAGCACCA GTTT-3' (299 bp); the sense and antisense primers for cyclin A were: 5'-TTAGGGAAATGGAGGTTA-3' and 5'-CAGAAAG TATTGGGTAAGAA-3', respectively. RT-PCR was performed on a Nexus Gradient Mastercycler (Eppendorf). The cycling conditions were: 94˚C for 2 min, followed by 30 cycles of 94˚C for 30 sec, 53-56˚C for 30 sec, and 72˚C for 1 min, and a final extension of 72˚C for 10 min. The PCR products were separated on 1.5% agarose gel and visualized by EB staining. The data were acquired with a Tocan 360 gel imager (version 3.2.1 software) (Shanghai Tiancheng Technology Co., Ltd., China).

Cell cycle analysis. HepG2 cells ($1x10^5$) were seeded in a 6-well plate and incubated for 24 h at 37˚C (5% CO_2), the medium was replaced with fresh medium, supplemented or not (control) with the agents (40 and 80 μM for PPAH, or 2.5 and 5 μM for the PPAH-Cu complex). After 24 h of incubation, the cells were harvested with trypsin, followed by washing with phosphate-buffered saline (PBS), fixed in 70% ethanol and stored at -20˚C. The cellular nuclear DNA was stained with propidium iodide (PI). Briefly, after removing the 70% ethanol, the cells were washed with PBS and then suspended in 0.5 ml PBS containing 50 μg/ml PI and 100 μg/ml RNase. The cell suspension was incubated at 37˚C for 30 min. DNA flow cytometry was performed in duplicate with a FACSCalibur flow cytometer (Becton-Dickinson, USA). For each sample 10,000 events were collected, and fluorescent signal intensity was recorded and analyzed by CellQuest and ModiFit (Becton-Dickinson).

DNA Top activity assay. The nuclear extract from HepG2 cells was prepared as previously described (15). The nuclear extract (0.4 μg) was added to the Top reaction mixture containing 10 mM Tris-HCl (pH 7.5), 1 mM EDTA, 150 mM NaCl, 0.1% bovine serum albumin (BSA), 5% glycerol and 0.4 μg pUC18 and 1 μl (or 2 or 3 μl) test agent (0.5 mM for PPAH or 0.3 mM for PPAH-Cu complex in water) at a final volume of 20 μl. Following incubation at 37˚C for 30 min, the reaction was terminated by adding 5 μl of stopping buffer (10% SDS, 0.025% bromophenol blue and 5% glycerol). The reaction products were analyzed by electrophoresis on 1% agarose gel using a TBE buffer with 0.1% SDS (89 mM Tris-HCl, 89 mM boric acid and 62 mM EDTA) at 45 V for 3 h, stained by EB (0.5 μg/ml) and photographed using a short wavelength UV lamp on a Tocan 360 gel scanner. The assay was conducted in duplicates.

Results

Determination of the molar ratio of PPAH/copper(II). PPAH has potential coordination atoms. Thus, in the presence of copper ions, a new species may be formed as a copper complex. To determine the molar ratio of PPAH to copper ions, the absorption spectra of varied concentrations of PPAH in water at a fixed copper concentration were recorded. As shown in Fig. 2, the copper(II) solution had no absorption in the investigated range of wavelength (240-400 nm). After

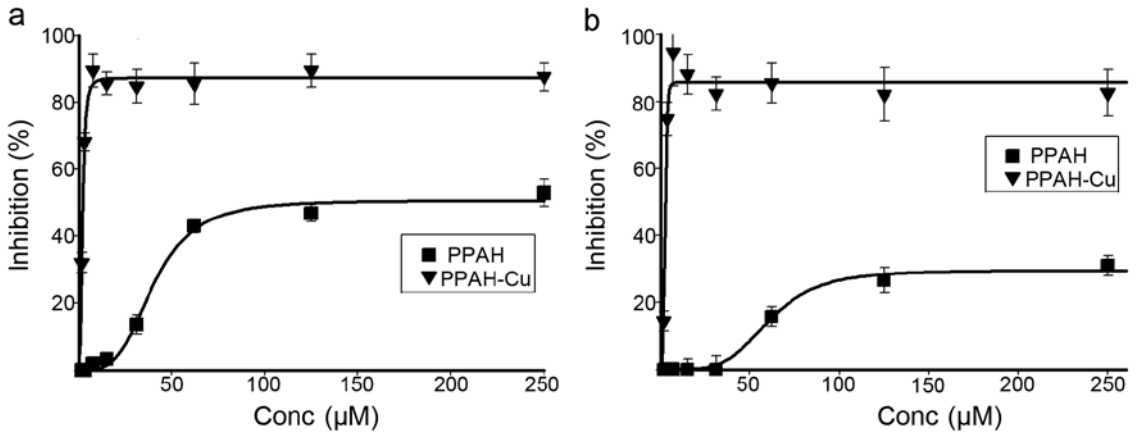

Figure 3. Inhibitory effect on cell proliferation of PPAH and its copper complex. (a) Inhibitory effect on cell proliferation of PPAH and its copper complex against HCT-116 cells; 50% at >60 μM for PPAH, 50% at 1.90±0.20 μM for the copper complex. (b) Inhibitory effect on cell proliferation of PPAH and its copper complex against HepG2 cells; 30% at 125 μM for PPAH and 50% at 2.75±0.30 μM for the copper complex. PPAH, 2-pyridinecarboxaldehyde 2-pyridinecarboxylic acid hydrazone.

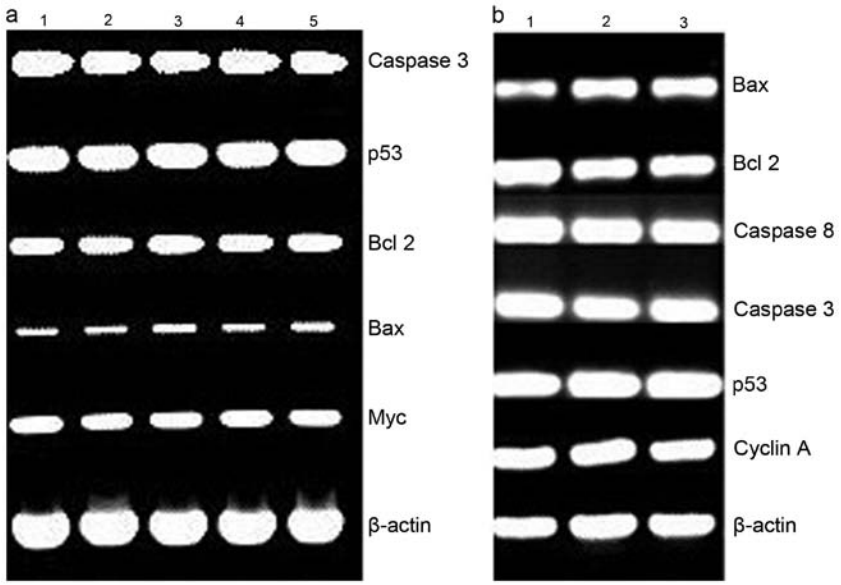

Figure 4. The gene regulation by PPAH and its copper complex (24 h incubation). (a) HepG2 cells were treated with the agents. Lane 1, 80 μM PPAH; lane 2, 40 μM PPAH; lane 3, control; lane 4, 2.5 μM PPAH-Cu complex; lane 5, 5 μM PPAH-Cu complex. (b) HCT-116 cells were treated with the PPAH-Cu complex. Lane 1, control (without PPAH-Cu complex); lane 2, 2.5 μM PPAH-Cu complex; lane 3, 5 μM PPAH-Cu complex. PPAH, 2-pyridinecarboxaldehyde 2-pyridinecarboxylic acid hydrazone.

addition of PPAH to the copper solution a new absorption at ~350 nm was noted, which was different from the PPAH absorption (~310 nm), indicating that a copper complex had formed. To further determine its composition, a series of solutions was prepared in which the concentration of $CuCl_2$ was held constant while that of the PPAH was varied. The absorbance of each solution was measured (Fig. 2a) and plotted vs. the molar ratio of Cu(II)/PPAH (Fig. 2b). From Fig. 2, a 1:1 molar ratio of Cu(II)/PPAH was determined. It was reported that the coordination geometry of 2-pyridinecarboxaldehyde benzoyl hydrazone with copper complexes has been described as a tridentate chelator (16). In view of the similarity of PPAH to the above ligand in chemistry, the structure of the PPAH copper complex was tentatively proposed (Fig. 1b).

Proliferation assay. To determine the potential antitumor activity of the agents, the inhibitory effects on the proliferation of the HepG2 and HCT-116 cell lines was investigated by MTT assay (Fig. 3). For both cell lines, the PPAH exhibited moderate inhibition of proliferation, i.e. 50% growth inhibition at ≥60 μM against HCT-116; ~30% growth inhibition at ≥100 μM against HepG2 (Fig. 3a and b). The copper complex exhibited excellent proliferation inhibition against the cell lines. The IC_{50} value of the copper complex was 2.75±0.30 μM for the HepG2 cells, an ~45-fold increase in proliferation inhibition compared to that of PPAH. A similar trend against the HCT-116 cell line was also observed. The IC_{50} value of the copper complex was 1.90±0.2 μM, an ~30-fold increase, which demonstrated that the copper complex exhibited excellent antitumor activity.

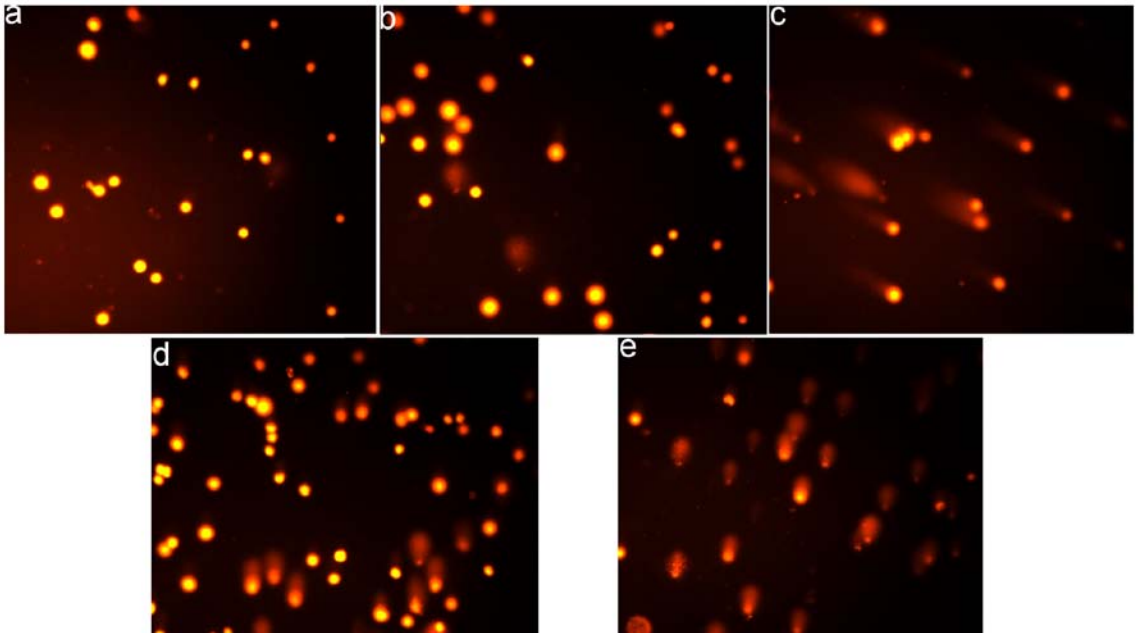

Figure 5. PPAH and its copper complex cause cellular DNA fragmentation. (a) Control, (b) 40 μM PPAH, (c) 80 μM PPAH, (d) 1.5 μM PPAH-Cu complex, and (e) 2.5 μM PPAH-Cu complex. The cells were treated with the agents for 48 h. PPAH, 2-pyridinecarboxaldehyde 2-pyridinecarboxylic acid hydrazone.

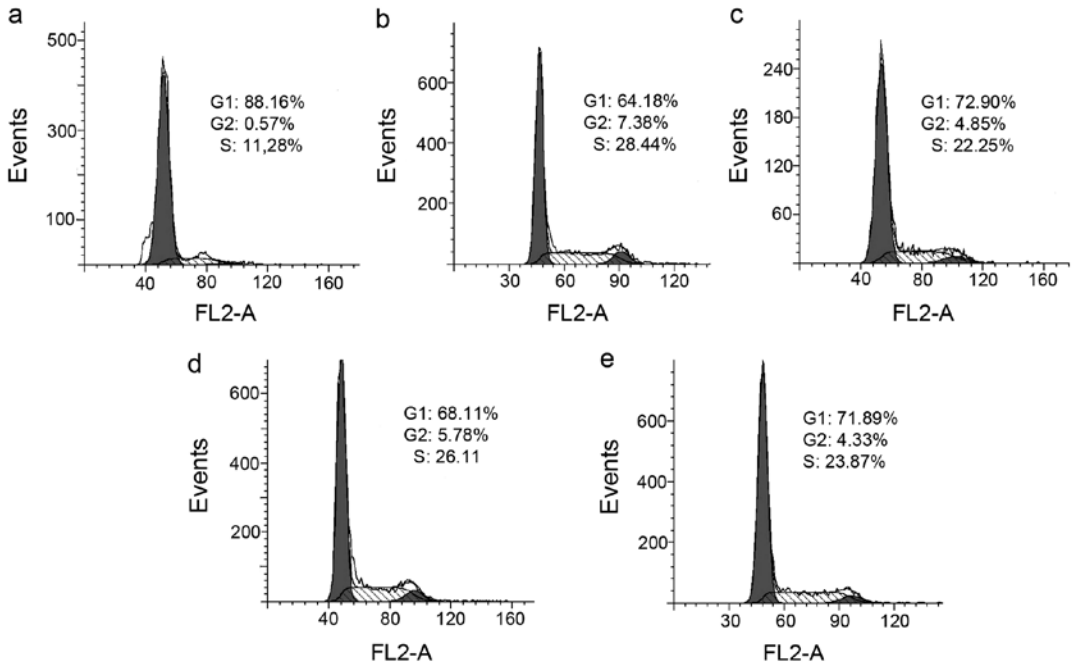

Figure 6. Cell cycle arrest by PPAH and its copper complex. (a) Control, (b) 40 μM PPAH, (c) 80 μM PPAH, (d) 2.5 μM PPAH-Cu complex, (e) 5 μM PPAH-Cu complex. PPAH, 2-pyridinecarboxaldehyde 2-pyridinecarboxylic acid hydrazone.

Effect of PPAH and its copper complex on the expression of apoptotic genes. ROS play a crucial role in cell growth and apoptosis. To reveal the mechanism of action of PPAH and its copper complex, RT-PCR was conducted to determine changes in expression of apoptotic genes, such as bcl-2, bax, p53, caspase-3 and -8 at the mRNA level after HepG2 cells were treated with PPAH (Fig. 4a) or its copper complex (Fig. 4b) for 48 h. The investigated genes were not evidently regulated by the agents. bcl-2 downregulation and bax upregulation were not observed, which normally occurs in ROS-related apoptosis. Similar analysis was conducted using the HCT-116 cell line. Except for PPAH due to its lesser toxicity, slight changes in the levels of the apoptosis-related genes were observed in the PPAH-Cu-treated cells. To ascertain whether ROS are involved in the proliferation inhibition, ROS production was investigated *in vitro*. The results indicated that the PPAH-Cu complex was non-redox active and did not lead to DNA fragmentation (data not shown). This was also consistent with the

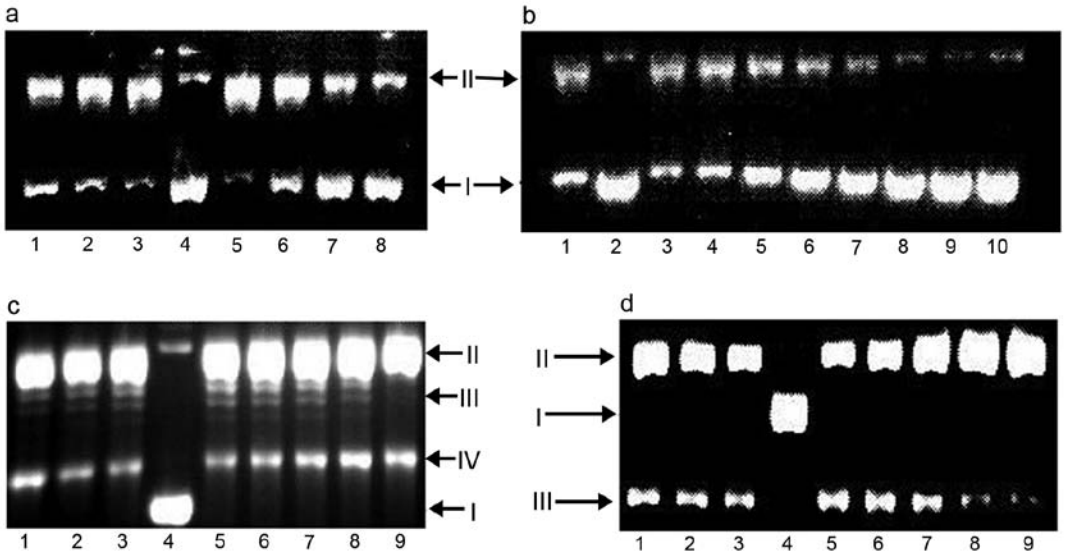

Figure 7. Top inhibition of PPAH and its copper complex. I, supercoiled DNA; II nicked DNA; III, relaxed DNA. (a) Lane 1, 150 μM PPAH; lane 2, 100 μM PPAH; lane 3, 50 μM PPAH; lane 4, pUC18; lane 5, pUC18 + NE; lane 6, 30 μM PPAH-Cu; lane 7, 60 μM PPAH-Cu; lane 8, 90 μM PPAH-Cu. (b) Lane 1, no PPAH; lane 2, pUC18; lane 3, 6 μM PPAH-Cu; lane 4, 12.5 μM PPAH-Cu; lane 5, 25 μM PPAH-Cu; lane 6, 50 μM PPAH-Cu; lane 7, 75 μM PPAH-Cu; lane 8, 100 μM PPAH-Cu; lane 9, 125 μM PPAH-Cu; lane 10, 150 μM PPAH-Cu. (c) Lane 1, 75 μM PPAH; lane 2, 50 μM PPAH; lane 3, 25 μM PPAH; lane 4, pUC18 only; lane 5, pUC18 and without investigated agent; lane 6, 12.5 μM PPAH-Cu; lane 7, 25 μM PPAH-Cu; lane 8, 37.5 μM PPAH-Cu; lane 9, etoposide control (3 mM). (d) Lane 1, 75 μM PPAH; lane 2, 50 μM PPAH; lane 3, 25 μM PPAH; lane 4, pUC18 only; lane 5, pUC18 and without investigated agent; lane 6, 12.5 μM PPAH-Cu; lane 7, 25 μM PPAH-Cu; lane 8, 37.5 μM PPAH-Cu; lane 9, etoposide (3 mM) control, electrophoresis in the presence of EB. PPAH, 2-pyridinecarboxaldehyde 2-pyridinecarboxylic acid hydrazone; EB, ethidium bromide.

results from the comet assay (Fig. 5). The DNA fragmentation was only observed at a higher concentration and 48 h exposure to PPAH and its copper complex.

PPAH and its copper complex induce S phase arrest. As shown above, ROS production was not correlated to the effect on inhibition of proliferation by PPAH and its copper complex. Thus, we hypothesized that they may exert their effect via disturbing the cell cycle. We therefore evaluated the effect of PPAH and its copper complex on the cell cycle using PI staining and flow cytometry. As shown in Fig. 6, PPAH caused an accumulation of cells in the S-phase. The percentage of cells in the S-phase was significantly increased from 11.22 to 28.44 and 22.25% after treatment with 40 and 80 μM PPAH, respectively. The PPAH-Cu complex had a similar effect when compared to PPAH; the S-phase population increased from 11.22 to 26.11 (2.5 μM) and 23.87% (2.5 μM), indicating that the agents have a similar mechanism of action that involves effects on the cell cycle except with differences at various concentrations.

DNA relaxation inhibition. Various transition metal complexes have Top inhibition. To determine whether PPAH and its copper complex recapitulate such activity, pUC18 plasmid DNA was incubated with nucleic extract in the presence of varied concentrations of the investigated agents, and reaction products were analyzed by gel electrophoresis. As shown in Fig. 7, PPAH exhibited very weaker inhibition even at a higher concentration (Top I, >100 μM; Top II >75 μM). The PPAH-Cu complex exhibited dual Top inhibition. For type I, a IC_{50} value of ~50 μM was noted; while type II inhibition was initialized at 12.5 μM (Fig. 7b and c). To further reveal the action mode of the copper complex in Top inhibition, the reaction mixtures were subjected to electrophoresis on EtB-containing agarose gel. As shown from the gel (Fig. 7d), the topology was dominated by the intercalative dye, all closed circular forms of DNA were positively supercoiled and migrated with a similar rate. The Top II cleavage complex was identified by comparison with the positive control of etoposide. However, in our experiment, the Top II cleavage complex was not observed. This situation may have occurred due to a lower Top II concentration used in the assay. The mode of Top inhibition of the PPAH-Cu complex was not clearly identified, but the cleaved DNA (Fig. 7d) increased with increasing concentrations of the copper complex implying that there was the possibility of catalytic or 'poisoner' inhibition.

Discussion

Pyridoxal isonicotinoyl hydrazone and Dp44mT have been extensively investigated for the treatment of different types of cancers and they are also considered as iron chelators as they disturb the homeostasis of this metal in cells. In terms of the mechanism, they are involved in iron deprivation and ROS enhancement (17,18). Although PPAH can enhance ROS generation and lead to DNA fragmentation in Fenton reaction, its cytotoxicity was found to be weak. In contrast, the PPAH-Cu complex displayed excellent antitumor activity. This seemingly contradictory phenomenon was reported for derivatives of 4-pyridine carboxylic acid hydrazide; Fe chelation efficacy is not always well correlated to the ability of a ligand to inhibit proliferation (19), indicating that ROS contributed less to their cytotoxicity. Comet assay has been widely used to evaluate ROS-induced DNA fragmentation. In the present study, cellular DNA fragmentation was only observed following a 48-h exposure of the agents, demonstrating that ROS were

less involved in the proliferation inhibition. To seek further evidence, RT-PCR was conducted to clarify whether the ROS were involved in the cell proliferation inhibition. As expected, the gene expression of bcl-2, bax, p53 and caspase at the mRNA level was not obviously changed following exposure of the agents for 24 or 48 h. It has been demonstrated that Bax and Bcl-2 are apoptosis-related genes and Bax upregulation and Bcl-2 downregulation are indicative of apoptosis (20,21). There were no changes in the investigated genes at the mRNA level which further suggested that proliferation inhibition by PPAH and its copper complex did not involve ROS generation.

Copper exhibits numerous biological processes as a co-factor of enzymes and angiopoiesis. A strategy using copper depletion therapy has been proposed to prevent the spread of cancers (22). Copper complexes have significant anticancer activity (23,24), yet the underlying mechanism is largely unknown. It has been reported that copper complexes induce cell death by causing double-strand DNA breakage and inhibition of Top function (25,26), thus the PPAH copper complex in the present study may share a similar mechanism of action. To test the hypothesis, DNA relaxation assay was carried out. It was found that the PPAH-Cu complex exhibited dual Top inhibition; type II Top inhibition was initiated at ~10 μM, while type I Top inhibition appeared to require a slightly higher dose (~40 μM). In contrast, PPAH had no obvious inhibitory effect, thus it could be speculated that the excellent antitumor activity of the PPAH-Cu complex may be closely correlated to its dual Top inhibition. Top inhibition by metal complexes has been reported in many studies. Metal complexes inhibited either Top I or Top II, such as 9-methyl-[1,10]phenanthroline-2-carboxylic acid cobalt complex (27), oxindolimine copper(II) complexes (28), organoplatinum(II) complexes (29) and Ru(II)-polypyridyl complexes (30). Yet, metal complexes acting as dual Top inhibitors are few. The PPAH-copper complex in the present study and ruthenium(II) anthraquinone complexes are the only two examples (31). It should be noted that the ligands were all fused aromatic compounds in the above mentioned metal complex, while in the present study PPAH was a simple pyridine derivative. There are many modes of interaction between Topoisomerases and their inhibitors, such as competitive ATP binding, poisoning DNA-Top covalent complex and allosteric effect on disturbing unwinding DNA helix. In the present study, the PPAH-Cu complex and etoposide appeared to possess similar action causing DNA cleavage; thus, the 'poisoner' of the Top II cleaved complex for the PPAH-Cu complex may be possible. Top inhibition normally leads to cell cycle arrest at the G2/M phase, yet S phase arrest was recently reported (32). The PPAH-Cu complex induced S-phase arrest at much lower concentrations that may be indicative of retarded DNA topology during DNA replication following exposure of the investigated agents. The PPAH-Cu complex was prepared in water and had excellent antitumor activity, yet PPAH-Fe^{2+} did not possess activity (data not shown), indicating that the geometry of the ligand induced by metal ions plays an important role in the inhibitory effect on cell proliferation.

In conclusion, the PPAH-Cu complex had significant proliferation inhibition compared to PPAH. The RT-PCR and comet assay indicated that ROS were less involved in the antitumor activity, yet the DNA relaxation assay provided new insight, revealing that the PPAH-Cu complex displayed dual Top inhibition in contrast to PPAH. Thus, the proliferation inhibition of the PPAH-Cu complex may mainly stem from its dual Top inhibition. Notably, Top inhibitors normally are coplanar aromatic compounds even in various metal complexes, and lack of fused aromatic cyclic compound as Top inhibitor is rare. Thus, the PPAH copper complex in the present study may be a novel dual Top inhibitor. However the detailed mechanism, particularly Top inhibition *in vivo*, and the interaction model between the copper complex and topoisomerase require further investigation.

Acknowledgements

This study was supported by grants (132102310250) from the Science and Technology Department of Henan Province and (2109901) from the Plan of Health Scientific and Technological Innovation Talents of Henan Province for S.L.

References

1. Chen Y and Hu L: Design of anticancer prodrugs for reductive activation. Med Res Rev 29: 29-64, 2009.
2. Chen Z, Zhang D, Yue F, Zheng M, Kovacevic Z and Richardson DR: The iron chelators Dp44mT and DFO inhibit TGF-β-induced epithelial-mesenchymal transition via up-regulation of N-Myc downstream-regulated gene 1 (NDRG1). J Biol Chem 287: 17016-17028, 2012.
3. Gupte A and Mumper RJ: Elevated copper and oxidative stress in cancer cells as a target for cancer treatment. Cancer Treat Rev 35: 32-46, 2009.
4. Pahl PM and Horwitz LD: Cell permeable iron chelators as potential cancer chemotherapeutic agents. Cancer Invest 23: 683-691, 2005.
5. Kalinowski DS, Sharpe PC, Bernhardt PV and Richardson DR: Structure-activity relationships of novel iron chelators for the treatment of iron overload disease: The methyl pyrazinylketone isonicotinoyl hydrazone series. J Med Chem 51: 331-344, 2008.
6. Chaston TB, Watts RN, Yuan J and Richardson DR: Potent antitumor activity of novel iron chelators derived from di-2-pyridylketone isonicotinoyl hydrazone involves Fenton-derived free radical generation. Clin Cancer Res 10: 7365-7374, 2004.
7. Filipović N, Borrmann H, Todorović T, Borna M, Spasojević V, Sladić D, Novaković I and Anđelković K: Copper(II) complexes of N-heteroaromatic hydrazones: Synthesis, X-ray structure, magnetic behavior, and antibacterial activity. Inorg Chim Acta 362: 1996-2000, 2009.
8. Hoyes KP, Hider RC and Porter JB: Cell cycle synchronization and growth inhibition by 3-hydroxypyridin-4-one iron chelators in leukemia cell lines. Cancer Res 52: 4591-4599, 1992.
9. Chaston TB and Richardson DR: Interactions of the pyridine-2-carboxaldehyde isonicotinoyl hydrazone class of chelators with iron and DNA: Implications for toxicity in the treatment of iron overload disease. J Biol Inorg Chem 8: 427-438, 2003.
10. Chaston TB, Lovejoy DB, Watts RN and Richardson DR: Examination of the antiproliferative activity of iron chelators: Multiple cellular targets and the different mechanism of action of triapine compared with desferrioxamine and the potent pyridoxal isonicotinoyl hydrazone analogue 311. Clin Cancer Res 9: 402-414, 2003.
11. Turner J, Koumenis C, Kute TE, Planalp RP, Brechbiel MW, Beardsley D, Cody B, Brown KD, Torti FM and Torti SV: Tachpyridine, a metal chelator, induces G_2 cell-cycle arrest, activates checkpoint kinases, and sensitizes cells to ionizing radiation. Blood 106: 3191-3199, 2005.
12. Fu Y, Zhou S, Liu Y, Yang Y, Sun X and Li C: The cytotoxicity of benzaldehyde nitrogen mustard-2-pyridine carboxylic acid hydrazone being involved in topoisomerase IIα inhibition. BioMed Res Int 2014: 527042, 2014.
13. Zheng X, Zhao Y and Zhu BX: Coordination of the new Schiff base with copper(II) or Iron(III) in solution. Wuji Huaxue Xuebao 27: 1523-1528, 2011 (In Chinese).

14. Singh NP, McCoy MT, Tice RR and Schneider EL: A simple technique for quantitation of low levels of DNA damage in individual cells. Exp Cell Res 175: 184-191, 1988.
15. Fu Y, Zhang Y, Zhou SF, Liu Y, Wang J, Wang Y, Lu C and Li C: The effects of substitution of carboxyl with hydrazide group on position 3 of ciprofloxacin on its antimicrobial and antitumor activity. Int J Pharm 9: 416-429, 2013.
16. Banerjee S, Sen S, Basak S, Mitra S, Hughes DL and Desplanches C: Two new pseudohalide-bridged Cu(II) complexes with a hydrazone ligand: Syntheses, crystal structures and magnetic studies. Inorg Chim Acta 361: 2707-2714, 2008.
17. Buss JL, Neuzil J and Ponka P: Oxidative stress mediates toxicity of pyridoxal isonicotinoyl hydrazone analogs. Arch Biochem Biophys 421: 1-9, 2004.
18. Jansson PJ, Hawkins CL, Lovejoy DB and Richardson DR: The iron complex of Dp44mT is redox-active and induces hydroxyl radical formation: An EPR study. J Inorg Biochem 104: 1224-1228, 2010.
19. Becker E and Richardson DR: Development of novel aroylhydrazone ligands for iron chelation therapy: 2-pyridylcarboxaldehyde isonicotinoyl hydrazone analogs. J Lab Clin Med 134: 510-521, 1999.
20. Gillardon F, Wickert H and Zimmermann M: Up-regulation of *bax* and down-regulation of *bcl-2* is associated with kainate-induced apoptosis in mouse brain. Neurosci Lett 192: 85-88, 1995.
21. Niu G, Yin S, Xie S, Li Y, Nie D, Ma L, Wang X and Wu Y: Quercetin induces apoptosis by activating caspase-3 and regulating Bcl-2 and cyclooxygenase-2 pathways in human HL-60 cells. Acta Biochim Biophys Sin 43: 30-37, 2011.
22. Turski ML and Thiele DJ: New roles for copper metabolism in cell proliferation, signaling, and disease. J Biol Chem 284: 717-721, 2009.
23. Jain S, Cohen J, Ward MM, Kornhauser N, Chuang E, Cigler T, Moore A, Donovan D, Lam C, Cobham MV, *et al*: Tetrathiomolybdate-associated copper depletion decreases circulating endothelial progenitor cells in women with breast cancer at high risk of relapse. Ann Oncol 24: 1491-1498, 2013.
24. Tardito S and Marchiò L: Copper compounds in anticancer strategies. Curr Med Chem 16: 1325-1348, 2009.
25. Skrott Z and Cvek B: Diethyldithiocarbamate complex with copper: The mechanism of action in cancer cells. Mini Rev Med Chem 12: 1184-1192, 2012.
26. Zhou BB and Elledge SJ: The DNA damage response: Putting checkpoints in perspective. Nature 408: 433-439, 2000.
27. Ahmad M, Afzal M, Tabassum S, Kalińska B, Mrozinski J and Bharadwaj PK: Synthesis and structure elucidation of a cobalt(II) complex as topoisomerase I inhibitor: In vitro DNA binding, nuclease and RBC hemolysis. Eur J Med Chem 74: 683-693, 2014.
28. Katkar P, Coletta A, Castelli S, Sabino GL, Couto RA, Ferreira AM and Desideri A: Effect of oxindolimine copper(II) and zinc(II) complexes on human topoisomerase I activity. Metallomics 6: 117-125, 2014.
29. Wang P, Leung CH, Ma DL, Lu W and Che CM: Organoplatinum(II) complexes with nucleobase motifs as inhibitors of human topoisomerase II catalytic activity. Chem Asian J 5: 2271-2280, 2010.
30. Gao F, Chao H and Ji LN: DNA binding, photocleavage, and topoisomerase inhibition of functionalized ruthenium(II)-polypyridine complexes. Chem Biodivers 5: 1962-1979, 2008.
31. Kou JF, Qian C, Wang JQ, Chen X, Wang LL, Chao H and Ji LN: Chiral ruthenium(II) anthraquinone complexes as dual inhibitors of topoisomerases I and II. J Biol Inorg Chem 17: 81-96, 2012.
32. Lin RW, Yang CN, Ku S, Ho CJ, Huang SB, Yang MC, Chang HW, Lin CM, Hwang J, Chen YL, *et al*: CFS-1686 causes cell cycle arrest at intra-S phase by interference of interaction of topoisomerase 1 with DNA. PLoS One 9: e113832, 2014.